Tripartite interactions between filamentous Pf4 bacteriophage, *Pseudomonas aeruginosa*, and bacterivorous nematodes

Caleb M. Schwartzkopf[1], Autumn J. Robinson[1], Mary Ellenbecker[1], Dominick R. Faith[1], Diane M. Brooks[1], Lincoln Lewerke[2], Ekaterina Voronina[1], Ajai A. Dandekar[2,3], and Patrick R. Secor[1#]

[1] Division of Biological Sciences, University of Montana, Missoula, Montana, USA
[2] Department of Microbiology, University of Washington, Seattle, Washington, USA
[3] Department of Medicine, University of Washington, Seattle, Washington, USA
[#] Correspondence: Patrick.secor@mso.umt.edu

Abstract

The opportunistic pathogen *Pseudomonas aeruginosa* PAO1 is infected by the filamentous bacteriophage Pf4. Pf4 virions promote biofilm formation, protect bacteria from antibiotics, and modulate animal immune responses in ways that promote infection. Furthermore, strains cured of their Pf4 infection (ΔPf4) are less virulent in animal models of infection. Consistently, we find that strain ΔPf4 is less virulent in a *Caenorhabditis elegans* nematode infection model. However, our data indicate that PQS quorum sensing is activated and production of the pigment pyocyanin, a potent virulence factor, is enhanced in strain ΔPf4. The reduced virulence of ΔPf4 despite high levels of pyocyanin production may be explained by our finding that *C. elegans* mutants unable to sense bacterial pigments through the aryl hydrocarbon receptor are more susceptible to ΔPf4 infection compared to wild-type *C. elegans*. Collectively, our data support a model where suppression of quorum-regulated virulence factors by Pf4 allows *P. aeruginosa* to evade detection by innate host immune responses.

Author Summary

Pseudomonas aeruginosa is an opportunistic bacterial pathogen that infects wounds, lungs, and medical hardware. *P. aeruginosa* strains are often themselves infected by a filamentous virus (phage) called Pf. At sites of infection, filamentous Pf virions are produced that promote bacterial colonization and virulence. Here, we report that strains of *P. aeruginosa* cured of their Pf infection are less virulent in a *Caenorhabditis elegans* nematode infection model. We also report that PQS quorum sensing and production of the virulence factor pyocyanin are enhanced in *P. aeruginosa* strains cured of their Pf infection. Compared to wild-type *C. elegans*, nematodes unable to detect bacterial pigments via the aryl hydrocarbon receptor AhR were more susceptible to infection by Pf-free *P. aeruginosa* strains that over-produce pyocyanin. Collectively, this study supports a model where Pf phage suppress *P. aeruginosa* PQS quorum sensing and reduce pyocyanin production, allowing *P. aeruginosa* to evade AhR-mediated immune responses in *C. elegans.*

Introduction

Filamentous bacteriophages (phages) of the Inoviridae family infect diverse bacterial hosts [1, 2]. In contrast to other phage families, Inoviruses can establish chronic infections where filamentous virions are produced without killing the bacterial host [3-5], which may allow a more symbiotic relationship between filamentous phages and the bacterial host to evolve. Indeed, filamentous phages are often associated with enhanced virulence potential in pathogenic bacteria. For example, the filamentous phage CTXϕ encodes the cholera toxin genes that convert non-pathogenic *Vibrio cholerae* into toxigenic strains [6], the MDAϕ Inovirus that infects *Neisseria gonorrhoeae* acts as a colonization factor and enhances bacterial adhesion to host tissues [7], and the filamentous phage ϕRSS1 increases extracellular polysaccharide production and invasive twitching motility in the plant pathogen *Ralstonia solanacearum* [8].

The filamentous phage Pf4 that infects *Pseudomonas aeruginosa* strain PAO1 enhances bacterial virulence in murine lung [9] and wound [10] infection models. Oxidative stress induces the Pf4 prophage [11] and filamentous virions are produced at high titers, up to 10^{11} virions per mL [12, 13]. Pf4 virions serve as structural components of biofilm matrices that protect bacteria from antibiotics and desiccation [9, 14, 15]. Pf4 virions also engage immune receptors on macrophages to decrease phagocytic uptake [10, 16] and inhibit CXCL1 signaling in keratinocytes, which interferes with wound re-epithelialization [17]. These observations outline the diverse ways that Pf4 virions promote the initiation and maintenance of *P. aeruginosa* infections. However, how Pf4 phages modulate bacterial virulence behaviors are poorly understood.

P. aeruginosa regulates the production of a variety of secreted virulence factors using a cell-to-cell communication system called quorum sensing (QS). As bacterial populations grow, concentrations of QS signaling molecules called autoinducers increase as a function of population density [18]. When autoinducer concentrations become sufficiently high, they bind to and activate their cognate receptors, allowing bacterial populations to coordinate gene expression [19, 20]. *P. aeruginosa* PAO1 has three QS systems, Las, Rhl, and PQS. Las and Rhl QS systems recognize acyl-homoserine lactone signals while the PQS system recognizes quinolone signals.

In this study, we demonstrate that deleting the Pf4 prophage from *P. aeruginosa*

PAO1 (ΔPf4) activates PQS quorum sensing and increases production of the pigment pyocyanin, a potent virulence factor. However, like observations in vertebrate infection models [9, 10], the virulence potential of ΔPf4 is reduced compared to PAO1 in a *Caenorhabditis elegans* nematode infection model. We resolve this apparent controversy and report that *C. elegans* strains lacking the ability to sense bacterial pigments through the aryl hydrocarbon receptor (AhR) are more susceptible to ΔPf4 infection compared to wild-type *C. elegans* capable of detecting bacterial pigments. Collectively, our data support a model where Pf4 suppresses the production of quorum-regulated pigments, allowing *P. aeruginosa* to evade detection by host immune responses.

Results

Pf4 protect *P. aeruginosa* from *Caenorhabditis elegans* predation

Prior work demonstrates that Pf4 enhances *P. aeruginosa* PAO1 virulence potential in mouse models of infection by modulating innate immune responses [9, 10, 16]. Because central components of animal innate immune systems are conserved, we hypothesized that Pf4 would affect *P. aeruginosa* virulence in other animals such as bacterivorous nematodes. To test this hypothesis, we used *Caenorhabditis elegans* nematodes in a slow-killing *P. aeruginosa* infection model were nematodes are maintained on minimal NNGM agar with a bacterial food source for several days [21].

We first confirmed that PAO1 and ΔPf4 grew equally well on NNGM agar without *C. elegans* (**Fig 1A**) by homogenizing and resuspending three-day-old bacterial lawns in saline and measuring colony forming units (CFUs) by drop-plate. Resuspended cells were then pelleted by centrifugation and Pf4 virions in supernatants were measured by plaque assay. In the absence of *C. elegans*, neither PAO1 nor Pf4 produced any detectable Pf4 virions (**Fig 1B**).

Subsequently, we tested the effect of *C. elegans* grazing on PAO1 and ΔPf4. Young adult N2 *C. elegans* were plated onto 24-hour old bacterial lawns and incubated for an additional 48 hours. In the presence of *C. elegans*, PAO1 CFUs were comparable to PAO1 CFUs recovered from lawns grown without *C. elegans* at approximately 10^{10} CFUs/mL (**Fig 1C**, black bar, compare to Fig 1A). CFUs recovered from ΔPf4 lawns

exposed to *C. elegans* were ~100-fold lower than ΔPf4 lawns grown without *C. elegans* (**Fig 1C**), indicating that Pf4 protects *P. aeruginosa* from *C. elegans* predation.

We did not detect Pf4 virions in ΔPf4 lawns exposed to *C. elegans* (**Fig 1D**), but we did recover ~1 x 10^6 Pf4 plaque forming units (PFUs) from PAO1 lawns exposed to *C. elegans* (**Fig 1D**, black bar). These results indicate that *C. elegans* induce Pf4 virion replication.

When filamentous Pf4 virions accumulate in the environment, they enhance *P. aeruginosa* adhesion to mucus and promote biofilm formation [14, 16]. Because *P. aeruginosa* colonization of the *C. elegans* digestive track is a primary cause of death in the slow killing model [21], we hypothesized that Pf4 virions may accumulate in the *C. elegans* digestive track. To test this hypothesis, we topically applied 1x10^9 fluorescently labeled Pf4 virions to bacterial lawns and imaged *C. elegans* by fluorescence microscopy after 24 hours of grazing. *Escherichia coli* OP50 were used for these experiments to avoid Pf4 replication and any potential bacterial lysis (Pf4 cannot *E. coli* hosts). After 24 hours, Pf4 virions accumulated in the upper intestine of *C. elegans* (**Fig 1E**), raising the possibility that Pf4 virions physically block the digestive track, which could increase *C. elegans* killing by *P. aeruginosa*.

When *C. elegans* was challenged with PAO1 in the slow killing model, nematode killing was complete after five days (**Fig 1F** black line) whereas complete *C. elegans* killing took eight days when challenged with ΔPf4 (**Fig 1F** green line), indicating that Pf4 enhances the virulence potential of *P. aeruginosa*, consistent with prior work in mice [9, 10, 16]. Collectively, these results indicate that *C. elegans* induces Pf4 replication and that Pf4 protects *P. aeruginosa* from *C. elegans* predation.

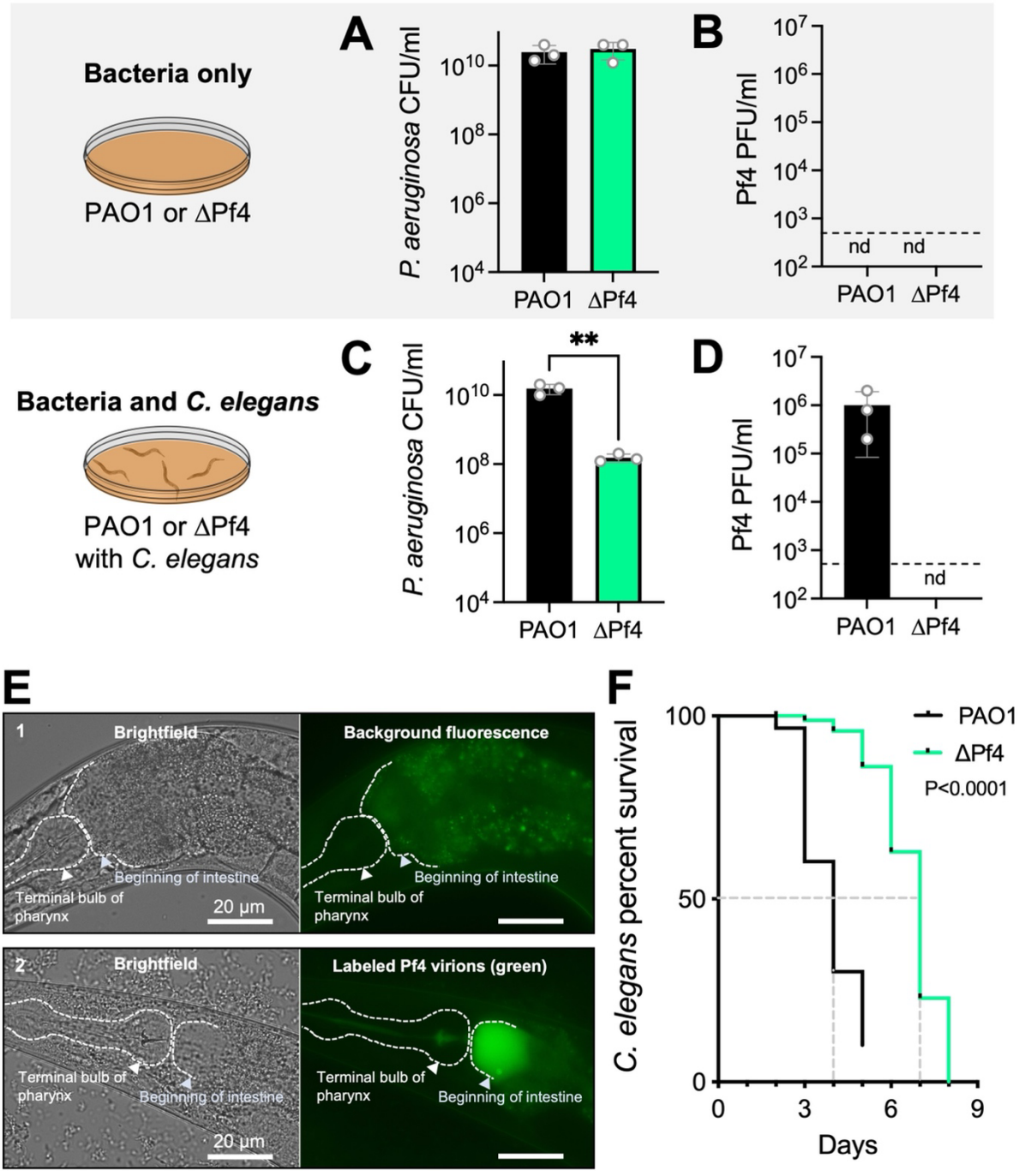

Figure 1. *C. elegans* predation induces Pf4 replication and enhances *P. aeruginosa* virulence. (A-D) Bacterial CFUs and Pf4 PFUs were enumerated after three days in the absence (A-B) or presence (C-D) of *C. elegans*. nd, not detected (below detection limit of 333 PFU/mL indicated by dashed line). Results are the mean ±SD of three experiments, **P<0.01, Student's *t*-test. **(E)** Wild-type N2 *C. elegans* were maintained on lawns of 1) *E. coli* OP50 (non-pathogenic nematode food) or 2) OP50 supplemented with 10^9 Pf4 virions labeled with Alexa-fluor 488 (green). Representative brightfield and fluorescent images after 24 hours are shown. **(F)** Kaplan-Meier survival curve analysis of *C. elegans* exposed to *P. aeruginosa*. N=90 worms per condition (three replicate experiments of 30 worms each). The mean survival of *C. elegans* maintained on

lawns of PAO1 was four days compared to seven days for nematodes maintained on lawns of ΔPf4 (dashed gray lines). Note that worms that may have escaped the dish rather than died were withdrawn from the study, explaining why the black PAO1 line does not reach zero percent survival.

PQS quorum sensing is activated and pyocyanin production enhanced in ΔPf4

During routine propagation of *P. aeruginosa*, we noted that production of the green pigment pyocyanin (**Fig 2A**) was significantly (P<0.003) higher in ΔPf4 compared to PAO1 (**Fig 2B and C**). Pyocyanin is a redox-active phenazine that shuttles electrons to distal electron acceptors, which enhances ATP production and generates proton-motive force in *P. aeruginosa* cells living in anoxic environments [22, 23]. The redox activity of pyocyanin also makes it a potent virulence factor that passively diffuses into phagocytes and kills them by redox cycling with NAD(H) to generate reactive oxygen species that indiscriminately oxidize cellular structures [24].

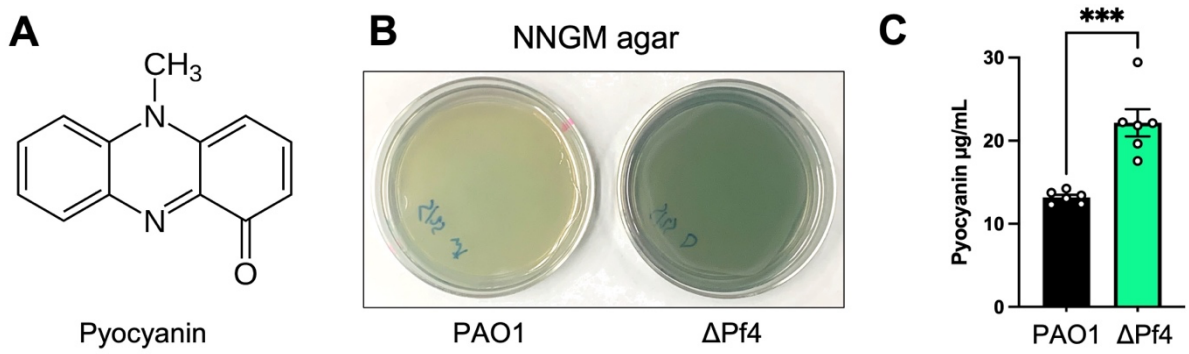

Figure 2. Pyocyanin production is enhanced in ΔPf4 compared to PAO1. (A) The structure of pyocyanin, a redox-active green pigment produced by *P. aeruginosa*. **(B)** Representative images of PAO1 and ΔPf4 growing on NNGM agar plates after 24 hours at 37°C. **(C)** Pyocyanin was chloroform-acid extracted from NNGM agar plates, absorbance measured (520 nm), and values converted to µg/mL. Data are the mean ±SEM of six replicate experiments. ***P<0.003, Student's *t*-test.

Expression of many *P. aeruginosa* virulence genes, including the phenazine biosynthesis genes responsible for pyocyanin production, are regulated by quorum sensing [25-32]. We used fluorescent transcriptional reporters to measure Las (P_{rsaL}::*gfp*), Rhl (P_{rhlA}::*gfp*), and PQS (P_{pqsA}::*gfp*) quorum sensing [33-35]. In ΔPf4, regulation of Las and Rhl gene targets was not significantly different from PAO1 after 18 hours of growth **(Fig 3A and B**). However, PQS activity in ΔPf4 was significantly (P<0.001) higher compared to PAO1 after 18 hours (**Fig 3C**). Fluorescence was not

169 detected in empty vector controls (**Fig 3D**). These results suggest that loss of the Pf4
170 prophage upregulates PQS quorum sensing, causing pyocyanin to be overproduced.
171

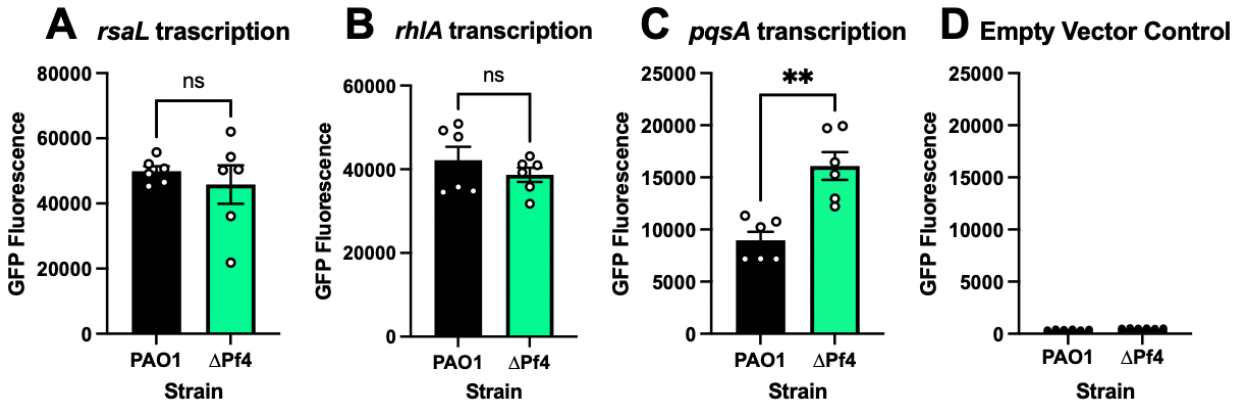

172
173 **Figure 3. PQS quorum sensing is upregulated in *P. aeruginosa* ΔPf4.** GFP fluorescence from
174 the transcriptional reporters (**A**) P_{rsaLI}-*gfp*, (**B**) P_{rhlA}-*gfp*, (**C**) P_{pqsA}-*gfp* and (**D**) P_{empty}-*gfp* was
175 measured in PAO1 (black) or ΔPf4 (green) at 18 hours in cultures growing in lysogeny broth. For
176 each measurement, GFP fluorescence was corrected for bacterial growth (OD_{600}). Data are the
177 mean ±SEM of six replicates. **P<0.001, Student's *t*-test.
178
179 Quantitative proteomics analysis of *C. elegans* exposed to PAO1 or ΔPf4

180 To gain insight into how Pf4 might affect *C. elegans* responses to *P. aeruginosa*,
181 we performed mass spectrometry-based quantitative proteomics on *C. elegans.* To
182 avoid progeny contamination, we used the *rrf-3(−); fem-1(−)* genetic background that is
183 sterile at temperatures above 25°C [36]. Like wild-type N2 nematodes, PAO1 killed the
184 *rrf-3(−); fem-1(−)* strain significantly (P<0.001) faster than ΔPf4 in the slow killing model
185 (**Fig S1**). Nematodes were maintained for two days on lawns of PAO1 or ΔPf4. This
186 timepoint was selected because most *C. elegans* were still alive in both groups (**Fig 1E;**
187 **Fig S1**). Whole nematodes were collected (~320 per replicate, N=4), washed, and
188 proteins purified (Methods). Proteins were digested with trypsin and tandem mass tags
189 were used to uniquely label peptides from each biological replicate, allowing all samples
190 to be pooled, fractionated, and analyzed by mass spectrometry in a single run. This
191 approach allows direct and quantitative comparisons between groups.
192

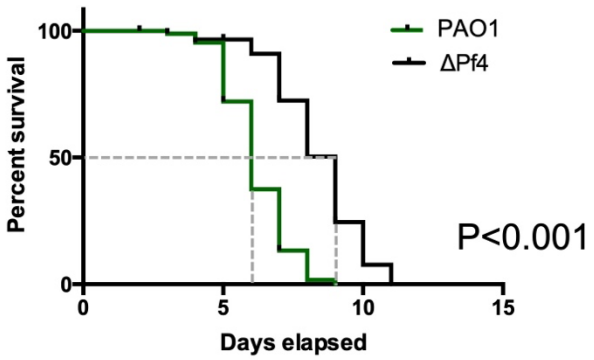

Figure S1. Survival analysis of sterile *rrf-3(-); fem-1(-) C. elegans* challenged with *P. aeruginosa* PAO1 or ΔPf4. Kaplan–Meier survival analysis of N=90 worms per condition (three replicate experiments of 30 worms each) were monitored daily for death. The mean survival of *rrf-3(-); fem-1(-) C. elegans* maintained on lawns of PAO1 was six days compared to nine days for nematodes maintained on lawns of ΔPf4 (dashed gray lines).

We identified 410 proteins that were significantly (P<0.05) up or down regulated at least 1.5-fold ($\log_2$ fold change ≥0.58) in *C. elegans* exposed to ΔPf4 compared to PAO1 (**Fig 4A, Supplemental Table S1**). Enrichment analysis revealed proteins associated with mitochondrial respiration and electron transport were significantly (FDR<0.002) enriched in upregulated proteins (**Fig 4B**). As pyocyanin is a redox-active virulence factor known to interfere with mitochondrial respiration [37, 38], these results suggest that respiration is perturbed in *C. elegans* grazing on ΔPf4 lawns that over-produce pyocyanin.

In *C. elegans* exposed to ΔPf4, proteins associated with the extracellular matrix (e.g., collagen) were also significantly enriched (**Fig 4A,** dark blue symbols; **Fig 4C**). The tough extracellular cuticle of *C. elegans* is composed predominantly of cross-linked collagen [39]. Because PAO1 kills *C. elegans* faster than ΔPf4 (**Fig 1E**), lower collagen abundance in PAO1-exposed *C. elegans* may be an indication of compromised cuticle integrity.

We also noted that proteins associated with muscle cell differentiation and organization were enriched in *C. elegans* challenged with ΔPf4 (**Fig 4D**), which could be related to a decline in motility observed in *C. elegans* as they begin to succumb to *P. aeruginosa* infection [21].

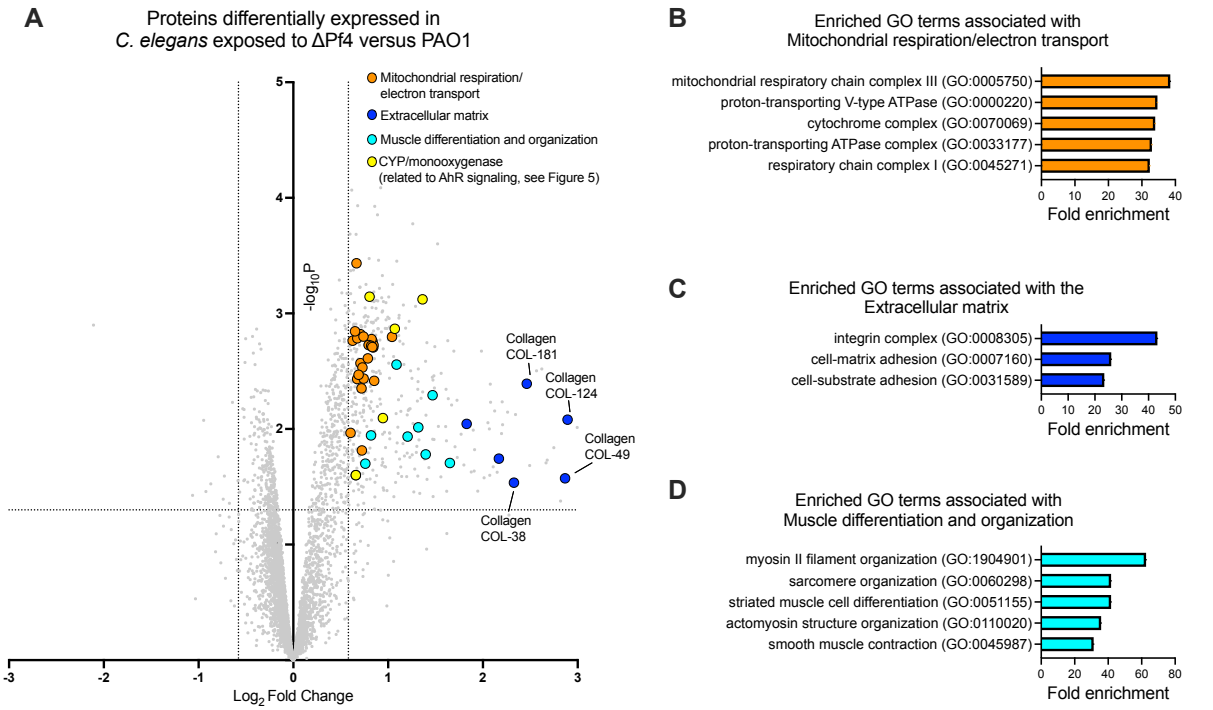

Figure 4. Pf4 modulates expression of *C. elegans* proteins associated with respiration, the extracellular matrix, and motility. (A) Volcano plot showing differentially expressed proteins in *C. elegans* maintained on lawns of ΔPf4 compared to *C. elegans* maintained on lawns of PAO1 for three days. The dashed lines indicate proteins with expression levels greater than ±1.5-fold and a false discovery rate (FDR) <0.05. Results are representative of quadruplicate experiments. **(B-D)** Enrichment analysis of significant upregulated proteins shown in (A). Fold enrichment of observed proteins associated with specific Gene Ontology (GO) terms each had an FDR of <0.002.

C. elegans aryl hydrocarbon receptor signaling regulates antibacterial defense

Compared to PAO1, ΔPf4 produces more of the virulence factor pyocyanin (and likely other quorum-regulated virulence factors). However, ΔPf4 is less virulent in mouse lung [9], wound [10], and *C. elegans* infection models (**Fig 1**). How is it that the ΔPf4 strain that produces more virulence factor is less virulent in animal models of infection?

Prior work demonstrates that vertebrate immune systems can sense *P. aeruginosa* aromatic pigments such as pyocyanin via the aryl hydrocarbon receptor (AhR) pathway [40, 41]. AhR is a highly conserved eukaryotic transcription factor that binds a variety of aromatic hydrocarbons and regulates metabolic processes that degrade xenobiotics and coordinate immune responses [40, 41]. In vertebrates, AhR's ability to detect pyocyanin and other bacterial pigments provides the host a way to monitor bacterial burden and mount appropriate immune countermeasures [41, 42].

241 Furthermore, AhR regulates the expression of numerous cytochrome P450
242 (CYP) enzymes in both vertebrates [43] and in *C. elegans* [44] that participate in
243 xenobiotic degradation. In our proteomics dataset, we identified five CYP proteins
244 (CYP-29a2, CYP-25a2, CYP-14a5, CYP-37a1, and CYP-35b1) that were significantly
245 upregulated in *C. elegans* exposed to ΔPf4 (**Fig 4A**, yellow symbols).
246 Based on these observations, we hypothesized that AhR signaling would
247 increase *C. elegans* fitness against the pyocyanin over-producing ΔPf4 strain. To test
248 this, we challenged wild-type N2 *C. elegans* or an AhR-null mutant (*ahr-1(ia3)*) with
249 PAO1 or ΔPf4 in the slow killing model. In wild-type nematodes, PAO1 was more
250 virulent than ΔPf4 (**Fig 5A,** solid lines), consistent with results shown in **Figure 1E**.
251 Survival curves of wild-type and *ahr-1(ia3) C. elegans* challenged with PAO1 were not
252 significantly different (**Fig 5B**, P=0.5664) and both had a median survival of four days
253 (**Fig 5C**, black bars). However, survival curves of wild-type and *ahr-1(ia3)* nematodes
254 challenged with ΔPf4 were significantly different (**Fig 5A,** dashed lines, P<0.0001) and
255 the median survival of wild-type verses *ahr-1(ia3)* decreased from seven to five days,
256 respectively (**Fig 5C**, green bars). These results indicate that *C. elegans* sensitivity to
257 infection by ΔPf4 is partially restored when AhR signaling is disabled.
258

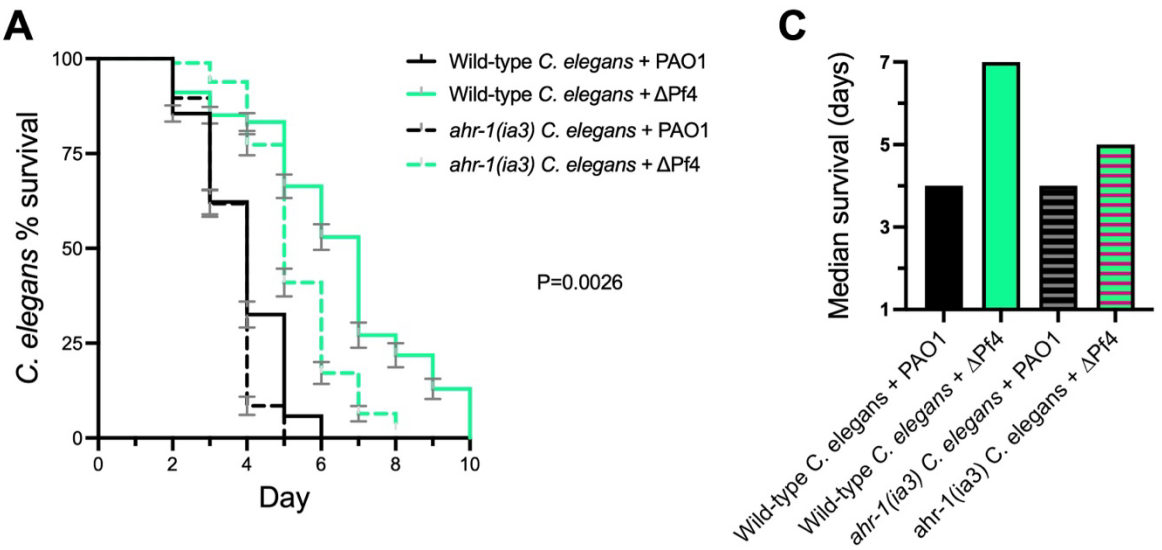

B

P -values from pairwise log-rank survival curve analyses

	Wild-type *C. elegans* + PAO1	Wild-type *C. elegans* + ΔPf4	*ahr-1(ia3) C. elegans* + PAO1	*ahr-1(ia3) C. elegans* + ΔPf4
Wild-type *C. elegans* + PAO1	–	P<0.0001	P=0.5664	P<0.0001
Wild-type *C. elegans* + ΔPf4		–	P<0.0001	P=0.0002
ahr-1(ia3) C. elegans + PAO1			–	P<0.0001
ahr-1(ia3) C. elegans + ΔPf4				–

Figure 5. Inactivation of AhR signaling in *C. elegans* enhances ΔPf4 virulence. (A) Kaplan-Meier survival curve analysis (Log-rank) of wild-type N2 or isogenic *ahr-1(ia3) C. elegans* maintained on lawns of *P. aeruginosa* PAO1 or ΔPf4 for the indicated times. N=3 groups of 90 animals per condition (270 animals total per condition). Error bars represent standard error of the mean. **(B)** P-values of pairwise log-rank survival curve analyses are shown. **(C)** The median survival of *C. elegans* in days was plotted for each group.

Discussion

Here, we characterize tripartite interactions between filamentous phage, pathogenic bacteria, and bacterivorous nematodes. Our work supports a model where Pf4 phage suppress *P. aeruginosa* PQS quorum sensing and reduce pyocyanin production, allowing *P. aeruginosa* to evade detection by AhR (**Fig 6**).

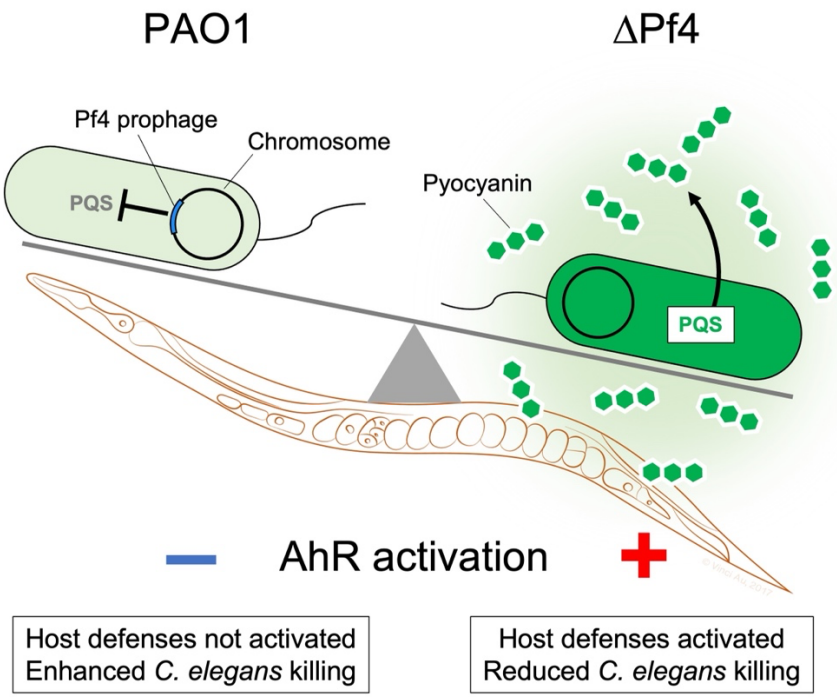

Figure 6. Proposed model. Pf4 suppresses the production of quorum-regulated pigments by *P. aeruginosa* allowing bacteria to evade AhR-mediated immune responses in *C. elegans*.

Many phages modulate bacterial quorum sensing systems [45, 46]. Examples in *P. aeruginosa* include phage DMS3, which encodes a quorum-sensing anti-activator protein called Aqs1 that binds to and inhibits LasR [47]. Another *P. aeruginosa* phage called LUZ19 encodes Qst, a protein that inhibits PQS signaling [48]. In both cases, it is thought that inhibition of *P. aeruginosa* quorum sensing makes the bacterial host more susceptible to phage infection.

Our finding that PQS signaling is upregulated when the Pf4 prophage is deleted suggests that Pf4 encodes proteins that inhibit PQS signaling, or that the phages themselves somehow suppress activation of the PQS circuit. The Pf4 prophage encodes a 5' retron element [49] and a 3' toxin-antitoxin pair [50] and these elements may be acting upon host quorum sensing systems. Another possible mechanism involves genes in the Pf core genome as there are still several with unknown function (e.g., *PA0717-PA0720*).

In the absence of *C. elegans*, PAO1 produces significantly less pyocyanin compared to ΔPf4 and infectious Pf4 virions are not simultaneously produced under these conditions. This indicates that the Pf4 prophage can modulate quorum-regulated

pigment production during lysogeny when infectious Pf4 virions are not produced. When *C. elegans* are present, however, Pf4 replication is induced and Pf4 virions appear to accumulate in the *C. elegans* intestine. Pf4 virions are known to promote *P. aeruginosa* biofilm formation and colonization of mucosal surfaces [14, 16, 51]. It is possible that Pf4 virions may contribute to *P. aeruginosa* colonization of the *C. elegans* intestine, which is a primary cause of *C. elegans* death in the slow killing model [21].

Our study had some limitations. For example, we only measured pyocyanin production by *P. aeruginosa*. Although pyocyanin is often used as an indicator of *P. aeruginosa* virulence potential [52, 53], there are many other factors that contribute to *P. aeruginosa* virulence, such as hydrogen cyanide [53]. We also only used well-defined laboratory strains of *P. aeruginosa* and *C. elegans*. While our study suggests that Pf phages may be broad modulators of bacterial virulence, to accurately predict how different *P. aeruginosa* strains (e.g., clinical vs environmental) might be affected by Pf, future work is required to characterize the effects various Pf strains have on QS systems in different *P. aeruginosa* hosts. One indication that Pf phages may behave differently in various bacterial hosts are variances in QS hierarchies in different *P. aeruginosa* isolates [54]. As quorum sensing can be rewired (e.g., Las dominant verses Rhl dominant hierarchies, [33, 55]), it would not be surprising that Pf phage modulate different behaviors in different *P. aeruginosa* hosts.

Our results support a role for AhR signaling in modulating *C. elegans* sensitivity to *P. aeruginosa* infection. Studies in vertebrates reveal that AhR serves as a pattern recognition receptor that senses aromatic bacterial pigments like pyocyanin to initiate appropriate immune responses [40, 41]. However, AhR recognizes a diverse array of ligands and modulation of inflammatory responses by AhR is context specific. For example, exposure of airway epithelial cells to combustion products induces pro-inflammatory AhR-dependent responses [56] while activation of AhR by tryptophan metabolites derived from commensal bacteria in the gut is associated with anti-inflammatory responses and maintenance of intestinal barrier integrity [57]. Our proteomics dataset and survival assays suggest that cuticle integrity might be compromised in *C. elegans* exposed to PAO1 compared to ΔPf4. An interesting research direction would be to link activation of AhR signaling by bacterial pigments to

enhanced cuticle integrity as a potential defense mechanism in nematodes.

In addition to AhR, *C. elegans* has other mechanisms to detect bacterial pigments. In environments illuminated with white light, *C. elegans* can discriminate the distinctive blue-green color of pyocyanin to avoid *P. aeruginosa* [58]. Our studies were performed predominantly in dark environments; future investigations on how Pf4 may affect *C. elegans* spectral sensing of pathogenic bacteria would be interesting. The existence of multiple bacterial pigment detection mechanisms in *C. elegans* highlights the importance of bacterial pigment detection in nematode survival.

Overall, our study provides evidence that Pf4 phage increase bacterial fitness against *C. elegans* predation. Prior work demonstrates that Pf4 phage also increase bacterial fitness against phagocytes by inhibiting bacterial uptake [10, 16]. In the environment, nematodes and other bacterivores such as phagocytic amoeba can impose high selective pressures on bacteria [59-61]. The ability of Pf phage to increase *P. aeruginosa* fitness against environmental bacterivores may help explain why Pf prophages are so widespread amongst diverse *P. aeruginosa* strains [3, 62, 63]. Further, the ability of Pf phage to increase bacterial fitness against bacterivores in the environment may translate to an enhanced ability of *P. aeruginosa* Pf lysogens to exploit opportunities to infect susceptible vertebrate hosts, such as people with medical implants, diabetic ulcers, or cystic fibrosis.

Materials and Methods:

Strains, plasmids, and growth conditions

Strains, plasmids, and their sources are listed in **Table 1.** Unless otherwise indicated, bacteria were grown in lysogeny broth (LB) at 37 °C with 230 rpm shaking and supplemented with antibiotics (Sigma) where appropriate. Unless otherwise noted, gentamicin was used at the at either 10 or 30 μg ml^{-1}.

Plaque assays

Plaque assays were performed using ΔPf4 as the indicator strain grown on LB plates. Phage in filtered supernatants were serially diluted 10x in PBS and spotted onto lawns of ΔPf4 strain. Plaques were imaged after 18h of growth at 37°C. PFUs/mL were then calculated.

Pyocyanin extraction and measurement

Pyocyanin was measured as described elsewhere [64, 65]. Briefly, 18-hour cultures were treated by adding chloroform to a total of 50% culture volume. Samples were vortexed vigorously and the different phases separated by centrifuging samples at 6,000xg for 5 minutes. The chloroform layer (dark blue if pyocyanin present) was removed to a fresh tube and 20% the volume of 0.1 N HCl was added and the mixture vortexed vigorously (if pyocyanin is present, the aqueous acid solution turns pink). Once the two layers were separated, the aqueous layer was removed to a fresh tube and absorbance measured at 520 nm. The concentration of pyocyanin in the culture supernatant, expressed as μg/ml, was obtained by multiplying the optical density at 520 nm by 17.072, as described [65].

Quorum sensing reporters

Competent *P. aeruginosa* PAO1 and ΔPf4 were prepared by washing overnight cultures in 300 mM sucrose followed by transformation by electroporation [66] with the plasmids CP1 Blank-PBBR-MCS5, CP53 PBBR1-MCS5 *pqsA*-gfp, CP57 PBBR1-MCS5 *rhlA*-gfp, CP59 PBBR1-MCS5 *rsaL*-gfp listed in **Table 1**. Transformants were selected by plating on the appropriate antibiotic selection media. The indicated strains were grown in buffered LB containing 50 mM MOPS and 100 μg ml^{-1} gentamicin for 18 hours. Cultures were then sub-cultured 1:100 into fresh LB MOPS buffer and grown to an OD_{600} of 0.3. To measure reporter fluorescence, each strain was added to a 96-well plate containing 200 μL LB MOPS with a final bacterial density of OD_{600} 0.1 and incubated at 37˚C in a CLARIOstar BMG LABTECH plate-reader. Prior to each measurement, plates were shaken at 230 rpm for a duration of two minutes. A measurement was taken every 15 minutes for both growth (OD_{600}) or fluorescence (excitation at 485-15 nm and emission at 535-15 nm).

Table 1. Bacterial strains, phage, and plasmids used in this study.

Strain	Description	Source
Escherichia coli		
DH5α	New England Biolabs	[67]
P. aeruginosa		
PAO1	Wild type	[9]
PAO1 ΔPf4	Deletion of the Pf4 prophage from PAO1	[9]
Bacteriophage Strains		
Pf4	Inovirus	[14]
C. elegans		
N2	Wild type	*Caenorhabditis* Genetic Center
ZG24	AhR null mutant *ahr-1(ia3)*	[68]
CF512	Temperature-sensitive sterile background *rrf-3(b26) II; fem-1(hc17) IV*	[36]
Plasmids		
CP59 pBBR1-MCS5 *rsaL-gfp*	GFP *lasI* transcriptional reporter	[35]
CP57 pBBR1-MCS5 *rhlA-gfp*	GFP *rhlA* transcriptional reporter	[35]
CP53 pBBR1-MCS5 *pqsA-gfp*	GFP *pqsA* transcriptional reporter	[34]
CP1 pBBR-MCS5-Blank	GFP empty vector control	[35]

C. elegans slow killing assay

Synchronized adult N2, *ahr-1(ia3),* or *rrf-3(-); fem-1(-) C. elegans* were plated on normal nematode growth media (NNGM) plates with 30 nematodes for each indicated lawn of *P. aeruginosa* and incubated at 30˚C. Over the course of the assay, nematodes were passaged onto new plates of 24-hour-old *P. aeruginosa* lawns daily and counted. Nematodes were counted as either alive or dead with missing nematodes being withdrawn from the study. The study was ended when all nematodes were either dead or missing.

Preparation of fluorescently tagged Pf4 virions

P. aeruginosa ΔPf4 was grown in LB broth to an OD_{600} of 0.5 at 37°C in a shaking incubator (225 rpm). Five µL of a Pf4 stock containing $5x10^9$ PFU/mL were used to infect the culture. After growing overnight (18h) in the 37°C shaking incubator, bacteria were removed by centrifugation (12,000 xg, 5 minutes, room temperature) and supernatants filtered through a 0.2 µm syringe filter. Pf4 virions were PEG precipitated by adding NaCl to the filtered supernatants to a final concentration of 0.5 M followed by the addition of PEG 8k to a final concentration of 20% w/vol. After incubating at 4°C for four hours, the supernatants became noticeably turbid. At this time, phage were pelleted by centrifugation (15,000 xg, 15 minutes, 4°C), the pellet gently washed in PBS, centrifuged again, and the phage pellet resuspended in 1 mL 0.1 M sodium bicarbonate

buffer, pH 8.3. Virions were then labeled with 100 µg of Alexa Fluor™ 488 TFP ester following the manufacturer's instructions (ThermoFisher). Unincorporated dyes were separated from labeled virions using PD-10 gel filtration columns. PBS was used to elute labeled phages from the column. Titers of labeled phages were measured by qPCR using our published protocol [69]. Labeled phages were aliquoted and stored at -20°C.

Fluorescent imaging of nematodes

Approximately 10^9 Alexa Fluor 488-labeled Pf4 virions in 200 µL PBS were added evenly to 24-hour old *E. coli* OP50 lawns growing on NNGM agar. Plates were incubated at 30°C for 30 minutes and synchronized adult N2 *C. elegans* were plated. Routine analysis of *C. elegans* by fluorescence/light microscopy was performed after 24 hours by transferring nematodes to a 5% agarose pad containing levamisole (250 mM), a nematode paralytic agent that enables imaging. Nematodes were examined and imaged using a Leica DFC300G camera attached to a Leica DM5500B microscope.

Protein extraction from *C. elegans*

Proteins were extracted from *rrf-3(-); fem-1(-) C. elegans* as described [70]. Briefly, after *P. aeruginosa* exposure for two days, ~320 *C. elegans* were harvested from NMMG plates into 1.5 mL tubes containing 1 mL PBS. Nematodes were gently mixed by hand, pelleted by centrifugation, and resuspended in 1 mL fresh PBS. *C. elegans* were again pelleted and supernatants were discarded, pellets were weighed and frozen at -80ºC until proteins were ready to be harvested. Pellets were suspended in reassembly buffer (RAB, 0.1M MES, 1mM EGTA, 0.1mM EDTA, 0.5mM $MgSO_4$, 0.75M NaCl, 0.2M NaF, pH7.4) containing Pierce Protease Inhibitor (ThermoScientific, A32965). Samples were sonicated on ice for 10 cycles of a 2 second pulse with 10 seconds rest between pulses. After 2 minutes rest, sonication was repeated for a total of 8 cycles of 10 x 2 second pulses. Lysates were centrifuged at 20,000xg for 30 minutes at 4ºC. Supernatants were transferred to fresh tubes and concentrated to approximately 2µg/µL using 10kDa molecular weight cut off spin columns (VivaSpin 500, Sartorius, VS0102). Protein concentration was determined using a Bradford assay. After visualizing protein integrity by SDS-PAGE (**Fig S2A**), 200 µg total protein for each of the four biological replicates for each treatment were sent to the IDeA National Resource for Quantitative Proteomics Center for proteomic analysis.

Mass spectrometry-based quantitative proteomics

Total protein (200 µg) from each sample was reduced, alkylated, and purified by chloroform/methanol extraction prior to digestion with sequencing grade modified porcine trypsin (Promega). Tryptic peptides were labeled using tandem mass tag isobaric labeling reagents (Thermo) following the manufacturer's instructions and

combined into one 16-plex TMTpro sample group. The labeled peptide multiplex was separated into 46 fractions on a 100 x 1.0 mm Acquity BEH C18 column (Waters) using an UltiMate 3000 UHPLC system (Thermo) with a 50 min gradient from 99:1 to 60:40 buffer A:B ratio under basic pH conditions, and then consolidated into 18 super-fractions. Each super-fraction was then further separated by reverse phase XSelect CSH C18 2.5 um resin (Waters) on an in-line 150 x 0.075 mm column using an UltiMate 3000 RSLCnano system (Thermo). Peptides were eluted using a 75 min gradient from 98:2 to 60:40 buffer A:B ratio. Eluted peptides were ionized by electrospray (2.4 kV) followed by mass spectrometric analysis on an Orbitrap Eclipse Tribrid mass spectrometer (Thermo) using multi-notch MS3 parameters. MS data were acquired using the FTMS analyzer in top-speed profile mode at a resolution of 120,000 over a range of 375 to 1500 m/z. Following CID activation with normalized collision energy of 35.0, MS/MS data were acquired using the ion trap analyzer in centroid mode and normal mass range. Using synchronous precursor selection, up to 10 MS/MS precursors were selected for HCD activation with normalized collision energy of 65.0, followed by acquisition of MS3 reporter ion data using the FTMS analyzer in profile mode at a resolution of 50,000 over a range of 100-500 m/z. Proteins were identified and quantified by database search using MaxQuant (Max Planck Institute) TMT MS3 reporter ion quantification with a parent ion tolerance of 2.5 ppm and a fragment ion tolerance of 0.5 Da. Buffer A = 0.1% formic acid, 0.5% acetonitrile. Buffer B = 0.1% formic acid, 99.9% acetonitrile. Both buffers were adjusted to pH 10 with ammonium hydroxide for offline separation.

Proteomics data analysis

Prior to data analysis, datasets (**Supplementary Table S1**) were subjected to and passed quality control procedures. To assess if there are more missing values than expected by random chance in one group compared to another, peptide intensity values were Log_2-transformed (**Fig S2B**). Peptide intensities were comparable across all groups. Principal component analysis (PCA) shows that biological replicates cluster within groups (**Fig S2C**).

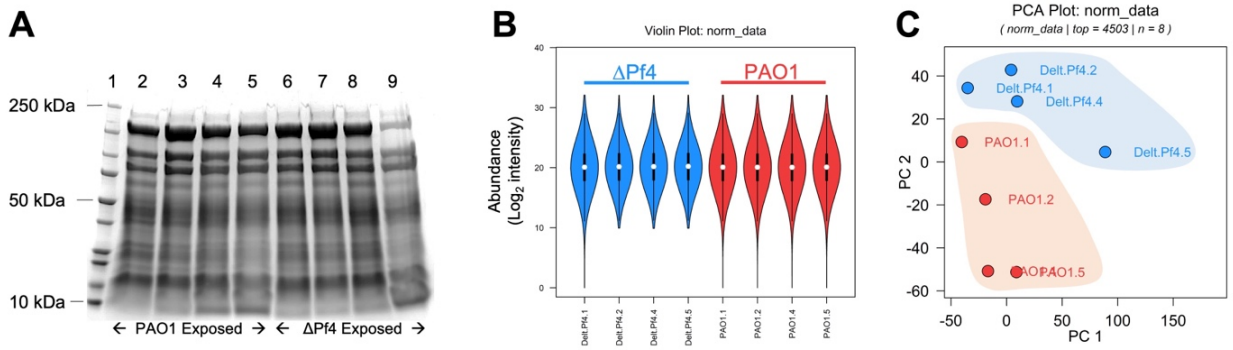

Figure S2. Protein input and proteomics data quality check. (A) *C. elegans* exposed to PAO1 or

ΔPf4 show similar total protein profiles. Forty-five µg of total protein extracted from *C. elegans rrf-3(-); fem-1(-)* exposed to either PAO1 or ΔPf4 for 48 hours was loaded onto a 4-15% Tris Glycine SDS gel and stained with Coomassie blue. Lane 1 Precision Plus All Blue Standard (Bio-Rad 1610373), Lanes 2-5 biological replicates of PAO1 exposed *C. elegans*, Lanes 6-9 ΔPf4 exposed *C. elegans*. Note that after sufficient protein was set aside for mass spectrometry analysis, protein for the sample in lane 9 was limiting, so less was loaded (~35 µg/µL). **(B)** Log_2 transformed peptide intensity values were comparable in all datasets. **(C)** Principal component analysis (PCA) shows that biological replicates cluster within groups.

The normalized Log_2 cyclic loess MS3 reporter ion intensities for TMT for the reference *P. aeruginosa* PAO1 proteome (UniprotKB: UP000002438) were compared between wild-type *P. aeruginosa* PAO1 and *P. aeruginosa* PAO1 ΔPf4 conditions. Proteins with ≥ 1.5-fold change (≥ 0.58 log_2FC) and P values < 0.05 were considered significantly differential. Functional classification and Gene Ontology (GO) enrichment analysis were performed using PANTHER classification system (http://www.pantherdb.org/) [71]. Analysis results were plotted with GraphPad Prism version 9.4.1 (GraphPad Software, San Diego, CA).

Statistical analyses

Differences between data sets were evaluated with a Student's *t*-test (unpaired, two-tailed) where appropriate. P values of < 0.05 were considered statistically significant. Survival curves were analyzed using the Kaplan–Meier survival analysis tool. Individual nematodes that were not confirmed dead were removed from the study. The Bonferroni correction for multiple comparisons was used when comparing individual survival curves. GraphPad Prism version 9.4.1 (GraphPad Software, San Diego, CA) was used for all analyses.

Acknowledgements

We thank Dr. Paul Bollyky and Dr. Laura Jennings for valuable discussions and critical reading of the manuscript. PRS is supported by NIH grants R01AI138981 and P20GM103546. AAD is supported by NIH grant R01GM125714. *C. elegans* strains were provided by the *Caenorhabditis* Genetics Center, which is funded by NIH Office of Research Infrastructure Programs (P40OD010440). The IDeA National Resource for Quantitative Proteomics Center is supported by NIH grant R24GM137786.

Conflicts of Interest

We declare no conflicts of interest.

References

1. Roux S, Krupovic M, Daly RA, Borges AL, Nayfach S, Schulz F, et al. Cryptic inoviruses revealed as pervasive in bacteria and archaea across Earth's biomes. Nat Microbiol. 2019. Epub 2019/07/25. doi: 10.1038/s41564-019-0510-x. PubMed PMID: 31332386.

2. Hay ID, Lithgow T. Filamentous phages: masters of a microbial sharing economy. EMBO Rep. 2019;20(6). Epub 2019/04/07. doi: 10.15252/embr.201847427. PubMed PMID: 30952693; PubMed Central PMCID: PMCPMC6549030.

3. Secor PR, Burgener EB, Kinnersley M, Jennings LK, Roman-Cruz V, Popescu M, et al. Pf Bacteriophage and Their Impact on Pseudomonas Virulence, Mammalian Immunity, and Chronic Infections. Front Immunol. 2020;11:244. Epub 2020/03/11. doi: 10.3389/fimmu.2020.00244. PubMed PMID: 32153575; PubMed Central PMCID: PMCPMC7047154.

4. Rakonjac J, Bennett NJ, Spagnuolo J, Gagic D, Russel M. Filamentous Bacteriophage: Biology, Phage Display and Nanotechnology Applications. Curr Issues Mol Biol. 2011;13(2):51-76. Epub 2011/04/20. PubMed PMID: 21502666.

5. Schmidt AK, Fitzpatrick AD, Schwartzkopf CM, Faith DR, Jennings LK, Coluccio A, et al. A Filamentous Bacteriophage Protein Inhibits Type IV Pili To Prevent Superinfection of Pseudomonas aeruginosa. MBio. 2022:e0244121. Epub 20220118. doi: 10.1128/mbio.02441-21. PubMed PMID: 35038902.

6. Waldor MK, Mekalanos JJ. Lysogenic conversion by a filamentous phage encoding cholera toxin. Science. 1996;272(5270):1910-4. Epub 1996/06/28. doi: 10.1126/science.272.5270.1910. PubMed PMID: 8658163.

7. Bille E, Meyer J, Jamet A, Euphrasie D, Barnier JP, Brissac T, et al. A virulence-associated filamentous bacteriophage of Neisseria meningitidis increases host-cell colonisation. PLoS Pathog. 2017;13(7):e1006495. Epub 2017/07/14. doi: 10.1371/journal.ppat.1006495. PubMed PMID: 28704569; PubMed Central PMCID: PMCPMC5526601.

8. Addy HS, Askora A, Kawasaki T, Fujie M, Yamada T. The filamentous phage varphiRSS1 enhances virulence of phytopathogenic Ralstonia solanacearum on tomato.

545 Phytopathology. 2012;102(3):244-51. doi: 10.1094/PHYTO-10-11-0277. PubMed PMID:
546 22085298.
547 9. Rice SA, Tan CH, Mikkelsen PJ, Kung V, Woo J, Tay M, et al. The biofilm life
548 cycle and virulence of Pseudomonas aeruginosa are dependent on a filamentous
549 prophage. Isme J. 2009;3(3):271-82. Epub 2008/11/14. doi: 10.1038/ismej.2008.109.
550 PubMed PMID: 19005496; PubMed Central PMCID: PMC2648530.
551 10. Sweere JM, Van Belleghem JD, Ishak H, Bach MS, Popescu M, Sunkari V, et al.
552 Bacteriophage trigger antiviral immunity and prevent clearance of bacterial infection.
553 Science. 2019;363(6434). Epub 2019/03/30. doi: 10.1126/science.aat9691. PubMed
554 PMID: 30923196.
555 11. JG H, A M-p, S K, D M, SA R. Environmental cues and genes involved in
556 establishment of the superinfective Pf4 phage of Pseudomonas aeruginosa. Front
557 Microbiol. 2014;5(654). doi: 10.3389/fmicb.2014.00654.
558 12. McElroy KE, Hui JG, Woo JK, Luk AW, Webb JS, Kjelleberg S, et al. Strain-
559 specific parallel evolution drives short-term diversification during Pseudomonas
560 aeruginosa biofilm formation. P Natl Acad Sci USA. 2014;111(14):E1419-27. Epub
561 2014/04/08. doi: 10.1073/pnas.1314340111. PubMed PMID: 24706926.
562 13. Webb JS, Lau M, Kjelleberg S. Bacteriophage and phenotypic variation in
563 Pseudomonas aeruginosa biofilm development. J Bacteriol. 2004;186(23):8066-73.
564 Epub 2004/11/18. doi: 10.1128/JB.186.23.8066-8073.2004. PubMed PMID: 15547279;
565 PubMed Central PMCID: PMC529096.
566 14. Secor PR, Sweere JM, Michaels LA, Malkovskiy AV, Lazzareschi D, Katznelson
567 E, et al. Filamentous Bacteriophage Promote Biofilm Assembly and Function. Cell Host
568 Microbe. 2015;18(5):549-59. Epub 2015/11/17. doi: 10.1016/j.chom.2015.10.013.
569 PubMed PMID: 26567508; PubMed Central PMCID: PMCPMC4653043.
570 15. Tarafder AK, von Kugelgen A, Mellul AJ, Schulze U, Aarts D, Bharat TAM. Phage
571 liquid crystalline droplets form occlusive sheaths that encapsulate and protect infectious
572 rod-shaped bacteria. Proc Natl Acad Sci U S A. 2020;117(9):4724-31. Epub
573 2020/02/20. doi: 10.1073/pnas.1917726117. PubMed PMID: 32071243; PubMed
574 Central PMCID: PMCPMC7060675.

16. Secor PR, Michaels LA, Smigiel KS, Rohani MG, Jennings LK, Hisert KB, et al. Filamentous Bacteriophage Produced by Pseudomonas aeruginosa Alters the Inflammatory Response and Promotes Noninvasive Infection In Vivo. Infect Immun. 2017;85(1). Epub 2016/11/01. doi: 10.1128/IAI.00648-16. PubMed PMID: 27795361; PubMed Central PMCID: PMCPMC5203648.

17. Bach MS, de Vries CR, Khosravi A, Sweere JM, Popescu MC, Chen Q, et al. Filamentous bacteriophage delays healing of Pseudomonas-infected wounds. Cell Rep Med. 2022;3(6):100656. doi: 10.1016/j.xcrm.2022.100656. PubMed PMID: 35732145.

18. Schuster M, Greenberg EP. A network of networks: quorum-sensing gene regulation in Pseudomonas aeruginosa. Int J Med Microbiol. 2006;296(2-3):73-81. Epub 2006/02/16. doi: 10.1016/j.ijmm.2006.01.036. PubMed PMID: 16476569.

19. Schuster M, Greenberg EP. A network of networks: quorum-sensing gene regulation in Pseudomonas aeruginosa. Int J Med Microbiol. 2006;296(2-3):73-81. Epub 2006/02/16. doi: 10.1016/j.ijmm.2006.01.036. PubMed PMID: 16476569.

20. Lee J, Zhang L. The hierarchy quorum sensing network in Pseudomonas aeruginosa. Protein Cell. 2015;6(1):26-41. Epub 2014/09/25. doi: 10.1007/s13238-014-0100-x. PubMed PMID: 25249263; PubMed Central PMCID: PMCPMC4286720.

21. Tan MW, Mahajan-Miklos S, Ausubel FM. Killing of Caenorhabditis elegans by Pseudomonas aeruginosa used to model mammalian bacterial pathogenesis. Proc Natl Acad Sci U S A. 1999;96(2):715-20. doi: 10.1073/pnas.96.2.715. PubMed PMID: 9892699; PubMed Central PMCID: PMCPMC15202.

22. Saunders SH, Tse ECM, Yates MD, Otero FJ, Trammell SA, Stemp EDA, et al. Extracellular DNA Promotes Efficient Extracellular Electron Transfer by Pyocyanin in Pseudomonas aeruginosa Biofilms. Cell. 2020;182(4):919-32 e19. Epub 2020/08/09. doi: 10.1016/j.cell.2020.07.006. PubMed PMID: 32763156; PubMed Central PMCID: PMCPMC7457544.

23. Glasser NR, Kern SE, Newman DK. Phenazine redox cycling enhances anaerobic survival in Pseudomonas aeruginosa by facilitating generation of ATP and a proton-motive force. Mol Microbiol. 2014;92(2):399-412. Epub 2014/03/13. doi: 10.1111/mmi.12566. PubMed PMID: 24612454; PubMed Central PMCID: PMCPMC4046897.

606 24. Lau GW, Hassett DJ, Ran H, Kong F. The role of pyocyanin in Pseudomonas
607 aeruginosa infection. Trends Mol Med. 2004;10(12):599-606. Epub 2004/11/30. doi:
608 10.1016/j.molmed.2004.10.002. PubMed PMID: 15567330.
609 25. Pesci EC, Milbank JBJ, Pearson JP, McKnight S, Kende AS, Greenberg EP, et
610 al. Quinolone signaling in the cell-to-cell communication system of Pseudomonas
611 aeruginosa. Proceedings of the National Academy of Sciences.
612 1999;96(20):11229-34. doi: doi:10.1073/pnas.96.20.11229.
613 26. Gallagher LA, McKnight SL, Kuznetsova MS, Pesci EC, Manoil C. Functions
614 Required for Extracellular Quinolone Signaling by Pseudomonas aeruginosa.
615 Journal of Bacteriology. 2002;184(23):6472-80. doi: doi:10.1128/JB.184.23.6472-
616 6480.2002.
617 27. Mukherjee S, Moustafa DA, Stergioula V, Smith CD, Goldberg JB, Bassler BL.
618 The PqsE and RhlR proteins are an autoinducer synthase-receptor pair that control
619 virulence and biofilm development in Pseudomonas aeruginosa. Proc Natl Acad Sci U S
620 A. 2018;115(40):E9411-E8. Epub 2018/09/19. doi: 10.1073/pnas.1814023115. PubMed
621 PMID: 30224496; PubMed Central PMCID: PMCPMC6176596.
622 28. Letizia M, Mellini M, Fortuna A, Visca P, Imperi F, Leoni L, et al. PqsE Expands
623 and Differentially Modulates the RhlR Quorum Sensing Regulon in Pseudomonas
624 aeruginosa. Microbiology Spectrum. 2022;10(3):e00961-22. doi:
625 doi:10.1128/spectrum.00961-22.
626 29. McKnight SL, Iglewski BH, Pesci EC. The Pseudomonas Quinolone
627 Signal Regulates rhl Quorum Sensing in Pseudomonas aeruginosa.
628 Journal of Bacteriology. 2000;182(10):2702-8. doi: doi:10.1128/JB.182.10.2702-
629 2708.2000.
630 30. Farrow III JM, Sund ZM, Ellison ML, Wade DS, Coleman JP, Pesci EC. PqsE
631 functions independently of PqsR-Pseudomonas quinolone signal and enhances the rhl
632 quorum-sensing system. Journal of bacteriology. 2008;190(21):7043-51.
633 31. Soto-Aceves MP, Cocotl-Yanez M, Servin-Gonzalez L, Soberon-Chavez G. The
634 Rhl Quorum-Sensing System Is at the Top of the Regulatory Hierarchy under
635 Phosphate-Limiting Conditions in Pseudomonas aeruginosa PAO1. J Bacteriol.

636 2021;203(5). Epub 20210208. doi: 10.1128/JB.00475-20. PubMed PMID: 33288622;
637 PubMed Central PMCID: PMCPMC7890550.
638 32. Dietrich LE, Price-Whelan A, Petersen A, Whiteley M, Newman DK. The
639 phenazine pyocyanin is a terminal signalling factor in the quorum sensing network of
640 Pseudomonas aeruginosa. Mol Microbiol. 2006;61(5):1308-21. Epub 2006/08/02. doi:
641 10.1111/j.1365-2958.2006.05306.x. PubMed PMID: 16879411.
642 33. Asfahl KL, Smalley NE, Chang AP, Dandekar AA. Genetic and Transcriptomic
643 Characteristics of RhlR-Dependent Quorum Sensing in Cystic Fibrosis Isolates of
644 Pseudomonas aeruginosa. mSystems. 2022;7(2):e0011322. Epub 20220411. doi:
645 10.1128/msystems.00113-22. PubMed PMID: 35471121; PubMed Central PMCID:
646 PMCPMC9040856.
647 34. Smalley NE, Schaefer AL, Asfahl KL, Perez C, Greenberg EP, Dandekar AA.
648 Evolution of the Quorum Sensing Regulon in Cooperating Populations of Pseudomonas
649 aeruginosa. MBio. 2022;13(1):e0016122. Epub 20220222. doi: 10.1128/mbio.00161-22.
650 PubMed PMID: 35294222; PubMed Central PMCID: PMCPMC8863103.
651 35. Feltner JB, Wolter DJ, Pope CE, Groleau MC, Smalley NE, Greenberg EP, et al.
652 LasR Variant Cystic Fibrosis Isolates Reveal an Adaptable Quorum-Sensing Hierarchy
653 in Pseudomonas aeruginosa. MBio. 2016;7(5). Epub 2016/10/06. doi:
654 10.1128/mBio.01513-16. PubMed PMID: 27703072; PubMed Central PMCID:
655 PMCPMC5050340.
656 36. Garigan D, Hsu AL, Fraser AG, Kamath RS, Ahringer J, Kenyon C. Genetic
657 analysis of tissue aging in Caenorhabditis elegans: a role for heat-shock factor and
658 bacterial proliferation. Genetics. 2002;161(3):1101-12. doi:
659 10.1093/genetics/161.3.1101. PubMed PMID: 12136014; PubMed Central PMCID:
660 PMCPMC1462187.
661 37. Manago A, Becker KA, Carpinteiro A, Wilker B, Soddemann M, Seitz AP, et al.
662 Pseudomonas aeruginosa pyocyanin induces neutrophil death via mitochondrial
663 reactive oxygen species and mitochondrial acid sphingomyelinase. Antioxid Redox
664 Signal. 2015;22(13):1097-110. Epub 20150318. doi: 10.1089/ars.2014.5979. PubMed
665 PMID: 25686490; PubMed Central PMCID: PMCPMC4403017.

666 38. O'Malley YQ, Abdalla MY, McCormick ML, Reszka KJ, Denning GM, Britigan BE.
667 Subcellular localization of Pseudomonas pyocyanin cytotoxicity in human lung epithelial
668 cells. Am J Physiol Lung Cell Mol Physiol. 2003;284(2):L420-30. Epub 20021101. doi:
669 10.1152/ajplung.00316.2002. PubMed PMID: 12414438.
670 39. Johnstone IL. Cuticle collagen genes. Expression in Caenorhabditis elegans.
671 Trends Genet. 2000;16(1):21-7. doi: 10.1016/s0168-9525(99)01857-0. PubMed PMID:
672 10637627.
673 40. Moura-Alves P, Fae K, Houthuys E, Dorhoi A, Kreuchwig A, Furkert J, et al. AhR
674 sensing of bacterial pigments regulates antibacterial defence. Nature.
675 2014;512(7515):387-92. Epub 2014/08/15. doi: 10.1038/nature13684. PubMed PMID:
676 25119038.
677 41. Moura-Alves P, Puyskens A, Stinn A, Klemm M, Guhlich-Bornhof U, Dorhoi A, et
678 al. Host monitoring of quorum sensing during Pseudomonas aeruginosa infection.
679 Science. 2019;366(6472). Epub 2019/12/21. doi: 10.1126/science.aaw1629. PubMed
680 PMID: 31857448.
681 42. Liu Y-C, Chan K-G, Chang C-Y. Modulation of host biology by Pseudomonas
682 aeruginosa quorum sensing signal molecules: messengers or traitors. Frontiers in
683 microbiology. 2015;6:1226.
684 43. Fujii-Kuriyama Y, Mimura J. Molecular mechanisms of AhR functions in the
685 regulation of cytochrome P450 genes. Biochem Biophys Res Commun.
686 2005;338(1):311-7. Epub 20050830. doi: 10.1016/j.bbrc.2005.08.162. PubMed PMID:
687 16153594.
688 44. Larigot L, Bui LC, de Bouvier M, Pierre O, Pinon G, Fiocca J, et al. Identification
689 of Modulators of the C. elegans Aryl Hydrocarbon Receptor and
690 Characterization of Transcriptomic and Metabolic AhR-1 Profiles. Antioxidants (Basel).
691 2022;11(5). Epub 20220523. doi: 10.3390/antiox11051030. PubMed PMID: 35624894;
692 PubMed Central PMCID: PMCPMC9137885.
693 45. Taylor VL, Fitzpatrick AD, Islam Z, Maxwell KL. The Diverse Impacts of Phage
694 Morons on Bacterial Fitness and Virulence. Adv Virus Res. 2019;103:1-31. Epub
695 2019/01/13. doi: 10.1016/bs.aivir.2018.08.001. PubMed PMID: 30635074.

696 46. Silpe JE, Bassler BL. Phage-Encoded LuxR-Type Receptors Responsive to
697 Host-Produced Bacterial Quorum-Sensing Autoinducers. MBio. 2019;10(2). Epub
698 2019/04/11. doi: 10.1128/mBio.00638-19. PubMed PMID: 30967469; PubMed Central
699 PMCID: PMCPMC6456758.
700 47. Shah M, Taylor VL, Bona D, Tsao Y, Stanley SY, Pimentel-Elardo SM, et al. A
701 phage-encoded anti-activator inhibits quorum sensing in Pseudomonas aeruginosa. Mol
702 Cell. 2021. Epub 2021/01/08. doi: 10.1016/j.molcel.2020.12.011. PubMed PMID:
703 33412111.
704 48. Hendrix H, Zimmermann-Kogadeeva M, Zimmermann M, Sauer U, De Smet J,
705 Muchez L, et al. Metabolic reprogramming of Pseudomonas aeruginosa by phage-
706 based quorum sensing modulation. Cell Rep. 2022;38(7):110372. doi:
707 10.1016/j.celrep.2022.110372. PubMed PMID: 35172131.
708 49. Mestre MR, González-Delgado A, Gutiérrez-Rus LI, Martínez-Abarca F, Toro N.
709 Systematic prediction of genes functionally associated with bacterial retrons and
710 classification of the encoded tripartite systems. Nucleic acids research.
711 2020;48(22):12632-47.
712 50. Li Y, Liu X, Tang K, Wang W, Guo Y, Wang X. Prophage encoding toxin/antitoxin
713 system PfiT/PfiA inhibits Pf4 production in Pseudomonas aeruginosa. Microb
714 Biotechnol. 2020;13(4):1132-44. Epub 2020/04/05. doi: 10.1111/1751-7915.13570.
715 PubMed PMID: 32246813; PubMed Central PMCID: PMCPMC7264888.
716 51. Secor PR, Jennings LK, Michaels LA, Sweere JM, Singh PK, Parks WC, et al.
717 Biofilm assembly becomes crystal clear - filamentous bacteriophage organize the
718 Pseudomonas aeruginosa biofilm matrix into a liquid crystal. Microb Cell. 2015;3(1):49-
719 52. Epub 2015/12/31. doi: 10.15698/mic2016.01.475. PubMed PMID: 28357315;
720 PubMed Central PMCID: PMCPMC5354590.
721 52. Alatraktchi FAa, Svendsen WE, Molin S. Electrochemical Detection of Pyocyanin
722 as a Biomarker for Pseudomonas aeruginosa: A Focused Review. Sensors.
723 2020;20(18):5218. PubMed PMID: doi:10.3390/s20185218.
724 53. Gallagher LA, Manoil C. Pseudomonas aeruginosa PAO1 kills Caenorhabditis
725 elegans by cyanide poisoning. J Bacteriol. 2001;183(21):6207-14. doi:

10.1128/JB.183.21.6207-6214.2001. PubMed PMID: 11591663; PubMed Central PMCID: PMCPMC100099.

54. Feltner JB, Wolter DJ, Pope CE, Groleau M-C, Smalley NE, Greenberg EP, et al. LasR Variant Cystic Fibrosis Isolates Reveal an Adaptable Quorum-Sensing Hierarchy in Pseudomonas aeruginosa. mBio. 2016;7(5):e01513-16. doi: doi:10.1128/mBio.01513-16.

55. Cruz RL, Asfahl KL, Van den Bossche S, Coenye T, Crabbe A, Dandekar AA. RhlR-Regulated Acyl-Homoserine Lactone Quorum Sensing in a Cystic Fibrosis Isolate of Pseudomonas aeruginosa. MBio. 2020;11(2). Epub 2020/04/09. doi: 10.1128/mBio.00532-20. PubMed PMID: 32265330; PubMed Central PMCID: PMCPMC7157775.

56. Martey CA, Baglole CJ, Gasiewicz TA, Sime PJ, Phipps RP. The aryl hydrocarbon receptor is a regulator of cigarette smoke induction of the cyclooxygenase and prostaglandin pathways in human lung fibroblasts. Am J Physiol Lung Cell Mol Physiol. 2005;289(3):L391-9. Epub 20050429. doi: 10.1152/ajplung.00062.2005. PubMed PMID: 15863442.

57. Scott SA, Fu J, Chang PV. Microbial tryptophan metabolites regulate gut barrier function via the aryl hydrocarbon receptor. Proc Natl Acad Sci U S A. 2020;117(32):19376-87. Epub 20200727. doi: 10.1073/pnas.2000047117. PubMed PMID: 32719140; PubMed Central PMCID: PMCPMC7431026.

58. Ghosh DD, Lee D, Jin X, Horvitz HR, Nitabach MN. C. elegans discriminates colors to guide foraging. Science. 2021;371(6533):1059-63. doi: 10.1126/science.abd3010. PubMed PMID: 33674494; PubMed Central PMCID: PMCPMC8554940.

59. Leong W, Poh WH, Williams J, Lutz C, Hoque MM, Poh YH, et al. Adaptation to an Amoeba Host Leads to Pseudomonas aeruginosa Isolates with Attenuated Virulence. Appl Environ Microbiol. 2022;88(5):e0232221. Epub 20220112. doi: 10.1128/aem.02322-21. PubMed PMID: 35020451; PubMed Central PMCID: PMCPMC8904051.

755 60. Hilbi H, Weber SS, Ragaz C, Nyfeler Y, Urwyler S. Environmental predators as
756 models for bacterial pathogenesis. Environ Microbiol. 2007;9(3):563-75. doi:
757 10.1111/j.1462-2920.2007.01238.x. PubMed PMID: 17298357.
758 61. Schulenburg H, Felix MA. The Natural Biotic Environment of Caenorhabditis
759 elegans. Genetics. 2017;206(1):55-86. doi: 10.1534/genetics.116.195511. PubMed
760 PMID: 28476862; PubMed Central PMCID: PMCPMC5419493.
761 62. Knezevic P, Voet M, Lavigne R. Prevalence of Pf1-like (pro)phage genetic
762 elements among Pseudomonas aeruginosa isolates. Virology. 2015;483:64-71. Epub
763 2015/05/13. doi: 10.1016/j.virol.2015.04.008. PubMed PMID: 25965796.
764 63. Fiedoruk K, Zakrzewska M, Daniluk T, Piktel E, Chmielewska S, Bucki R. Two
765 Lineages of Pseudomonas aeruginosa Filamentous Phages: Structural Uniformity over
766 Integration Preferences. Genome Biol Evol. 2020;12(10):1765-81. doi:
767 10.1093/gbe/evaa146. PubMed PMID: 32658245; PubMed Central PMCID:
768 PMCPMC7549136.
769 64. Kurachi M. Studies on the Biosynthesis of Pyocyanine.(I): On the Cultural
770 Condition for Pyocyanine Formation. Bulletin of the Institute for Chemical Research,
771 Kyoto University. 1958;36(6):163-73.
772 65. Essar DW, Eberly L, Hadero A, Crawford IP. Identification and characterization of
773 genes for a second anthranilate synthase in Pseudomonas aeruginosa:
774 interchangeability of the two anthranilate synthases and evolutionary implications.
775 Journal of Bacteriology. 1990;172(2):884-900. doi: doi:10.1128/jb.172.2.884-900.1990.
776 66. Choi K-H, Kumar A, Schweizer HP. A 10-min method for preparation of highly
777 electrocompetent Pseudomonas aeruginosa cells: application for DNA fragment transfer
778 between chromosomes and plasmid transformation. Journal of microbiological methods.
779 2006;64(3):391-7.
780 67. Castang S, Dove SL. Basis for the essentiality of H-NS family members in
781 Pseudomonas aeruginosa. J Bacteriol. 2012;194(18):5101-9. Epub 2012/07/24. doi:
782 10.1128/JB.00932-12. PubMed PMID: 22821971; PubMed Central PMCID:
783 PMC3430348.

784 68. Qin H, Powell-Coffman JA. The Caenorhabditis elegans aryl hydrocarbon
785 receptor, AHR-1, regulates neuronal development. Dev Biol. 2004;270(1):64-75. doi:
786 10.1016/j.ydbio.2004.02.004. PubMed PMID: 15136141.
787 69. Burgener EB, Secor PR, Tracy MC, Sweere JM, Bik EM, Milla CE, et al. Methods
788 for Extraction and Detection of Pf Bacteriophage DNA from the Sputum of Patients with
789 Cystic Fibrosis. Phage. 2020;1(2):100-8. Epub 2020/07/07. doi:
790 10.1089/phage.2020.0003. PubMed PMID: 32626852; PubMed Central PMCID:
791 PMCPMC7327540.
792 70. King CD, Singh D, Holden K, Govan AB, Keith SA, Ghazi A, et al. Proteomic
793 identification of virulence-related factors in young and aging C. elegans infected with
794 Pseudomonas aeruginosa. J Proteomics. 2018;181:92-103. Epub 20180412. doi:
795 10.1016/j.jprot.2018.04.006. PubMed PMID: 29656019.
796 71. Thomas PD, Ebert D, Muruganujan A, Mushayahama T, Albou LP, Mi H.
797 PANTHER: Making genome-scale phylogenetics accessible to all. Protein Sci.
798 2022;31(1):8-22. Epub 20211125. doi: 10.1002/pro.4218. PubMed PMID: 34717010;
799 PubMed Central PMCID: PMCPMC8740835.
800